



Characterization of lignin and derivative chars by infrared spectroscopy

Saloua Sebbahi*¹, Laila El fakir¹, Lotfi Rghioui², Afaf El Hajji¹, Younes Brik³, Fatima Kifani-Sahban⁴ and Souad El Hajjaji¹

¹Spectroscopy, Molecular Modeling, Materials and Environment Laboratory, Department of Chemistry, Faculty of Sciences B.P. 1014, Rabat, Morocco.

²Physicochemical team of condensed mater, Department of Chemistry, Faculty of Sciences. Meknes, Morocco.

³National Laboratory of Control of Medicament, Rabat Morocco

⁴Laboratory of Thermodynamic and Energetic, Physical department, Faculty of Sciences B.P. 1014, Rabat, Morocco.

Received 17 Jul 2015, Revised 05 Sep 2015, Accepted 09 Sep 2015

*Corresponding author: sebbahi_seloua@yahoo.fr

Abstract

This work deals with the spectroscopic characterization by attenuated total reflection (ATR) of lignin and derivative chars. The char is obtained by carbonizing the lignin. The char is then either directly activated or treated in air at 140°C and 245°C before being activated. The carbonization is carried out under nitrogen at 600°C and the activation under CO₂ at 700°C. The effect of the different heat treatments on the surface functional groups have been examined.

The oxygenated groups initially present in lignin are the aliphatic and cyclic ether, carbonyl, methoxyl, phenolic hydroxyl, primary and secondary aliphatic hydroxyl groups. These groups undergo a substantial loss during the carbonization except the cyclic ether group. Carbonization leads to a decrease in aliphaticity and an increase in aromaticity and the development of a thermoplastic phase by crazing. The band intensity of the various aforementioned oxygenated groups increases during the pre-treatment of coal by air. The pre-treatment in air also leads to the reformation of the carbonyl group. The presence of such groups and the increase in the pre-treatment temperature is reflected by a decrease of the thermoplastic character of the material. The carbonyl groups are formed during the activation of the raw char while they disappear during the activation of the pre-treated char in air before activation. Images taken by transmission electron microscopy (TEM) show the development of the microporosity in the first case and the plastic phase in the latter.

Keywords: Lignin; Carbonization; Air pre-oxidation; CO₂ activation; ATR infrared spectra; Surface chemistry; Oxygenated functional groups.

1. Introduction

The characterization of activated carbon is required to justify the scope of their application, among other surface chemistry. This latter determines the moisture content, the catalytic properties, the acid-base character and the adsorption capacity of activated carbon [1, 2]. The surface chemistry of the activated carbon is related to the presence of heteroatoms such as oxygen, hydrogen and nitrogen in the carbon matrix [1, 2]. The chemical properties of the surface of the activated carbon depends on the conditions in which it was prepared, including the stage of carbonization and activation when it is a physical activation.

It is in this context that our contribution will be made. In our previous work, activated carbon was prepared from lignin by physical activation. We showed that lignin undergoes plastic deformation during carbonization [3, 4]. The formation of this phase provides the char thermal stability during activation [4-6]. To reduce this stability, the char is treated in air at temperatures below 400°C before activation [4, 7, 8]. This operation affects the physical properties of char including its thermoplasticity, its chemical composition, its surface chemistry, and its reactivity during the activation and on the pore structure of activated carbon [4, 9-11].

In addition, we examined the effects of pre-oxidation conditions in air and activation conditions in the presence of CO₂ on some physical and physico-chemical characteristics of obtained chars. The technics employed for this purpose are the elemental analysis, specific surface area measurements, analysis by scanning electron microscope (SEM) and measurements of dimensional variations [4]. The objective of this work is to follow the evolution of oxygen functional groups on the surface after carbonization of lignin, after pre-

oxidation of lignin char in air and after activation with and without or not of the pretreatment. This characterization is performed using infrared spectroscopy by reflection mode (ATR).

2. Experimental part

2.1. Characteristics of lignin char

In this work, we used commercial lignin in its powder form (Aldrich, France). The lignin char was obtained after carbonization. The carbonization of lignin was carried out in a tubular furnace under flowing nitrogen of 30 cm³/min at a heating rate of 10°C/min. The temperature of carbonization was of 600°C and the residence time of the carbonaceous residue at this temperature was 2 hours. The coal thus prepared was called CL600. The elemental analysis of the lignin char was carried out with a Perkin Elmer 2400 CNH. The results were given in table 1.

Table 1: Elemental analysis of the lignin char

% C	% H	% O	% N
75.76	2.16	15.29	0.35

2.2. Procedure of pre-oxidation

The samples of CL600 are pre-oxidized under an air flow rate of 24 cm³/min in the furnace where the carbonization is carried out. The duration of the pre-treatment is 6 hours and pre-oxidation temperatures are 140°C and 245°C. The samples obtained under these conditions are respectively called CL600(140°C,6h,air) and CL600(245°C,6h,air). The choice of the duration and the aforementioned temperatures is the subject of a previous work [4].

2.3. Procedure of activation

The samples of CL600 pre-oxidized or not are gasified in the presence of CO₂. The flow of this last is of 24 cm³/min. The samples thus obtained are respectively called CL600(245°C,6h,air)(700°C,1h,CO₂) and CL600(700°C,1h,CO₂). The sample whose mass is approximately 100 mg, is heated under nitrogen up to the temperature of activation. Once that the temperature of activation is reached and remains constant, the nitrogen is stopped and CO₂ is introduced into the furnace. The activation temperature is 700°C and the time is 1 hour. The pre-oxidation is carried out at 245°C in air for 6 hours. At the end of the reaction, cooling is carried out under nitrogen. Similarly, the choice of the temperature and the time of activation has been a subject of a previous work [4].

2.4. Description of ATR

ATR infrared spectroscopy was used as a structural, nondestructive and simple tool for the qualitative analysis of the chemical composition of lignin and lignin which has undergone different treatments. The infrared spectra recordings were performed on a Bruker-Tensor 27 device using an Attenuated Total Reflection unit (ATR). The samples do not require any preliminary preparation. It is only enough to place a sufficient quantity of the sample (a few milligrams) on the attenuated total reflectance element. This element is, in our case, the germanium crystal, which allows acquisition between 4000 and 600 cm⁻¹ in wave number, then apply pressure and finally record the spectra.

2.5. Characterization by transmission electron microscope TEM

The TEM images were taken on a fine powder using a TECNAI G2 / FEI equipment with a CCD camera. The resolution is 0.35 nm and the expansion ranges from 150 to 500000x.

2.6. X-ray diffraction characterization

The powder diagram of lignin char was recorded with a D5000 Siemens type diffractometer using the K α_1 diffraction line of copper ($\lambda = 1.5406 \text{ \AA}$).

3. Results and discussion

The assignment proposed for the fundamental vibrations of lignin, lignin char and different treatments of this char are summarized in table 2. This assignment was made on the basis of previous works on the compounds of the same family [8-37].

3.1. Effect of carbonization

A typical structure of lignin is shown in figure 1. Figure 2 includes the infrared spectra of raw lignin and lignin char (CL600). The spectrum of the raw lignin has a strong wide band between 3685 and 3027 cm^{-1} . It is centered at 3410 cm^{-1} and corresponds to $\nu_{\text{ass}}(\text{O-H})$ stretching vibrations. This band is caused by presence of alcoholic and phenolic hydroxyl groups [24-26, 28, 29, 34]. The thin absorption with medium intensity observed at 1417 cm^{-1} is related to the vibration of deformation in plane $\delta(\text{O-H})$ of phenolic hydroxyl groups [25, 29]. The thin and weak band at 667 cm^{-1} corresponds to the out-of-plane deformation $\gamma(\text{O-H})$ of primary and secondary aliphatic hydroxyl groups and phenolic hydroxyl groups [29].

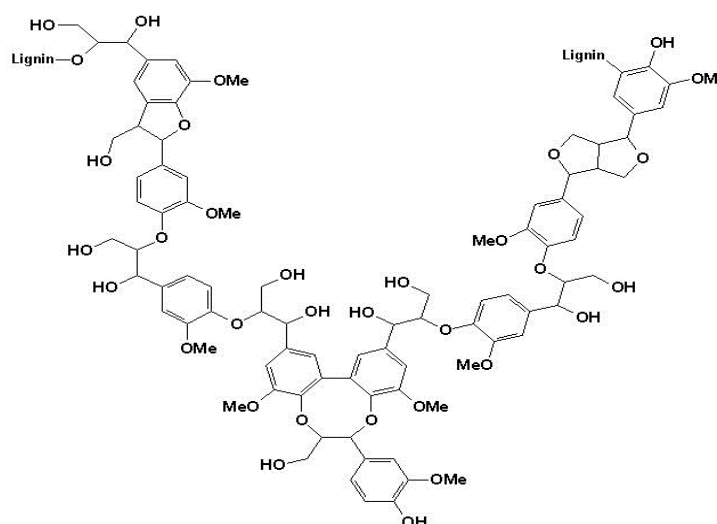


Figure 1. : A proposed structure of lignin

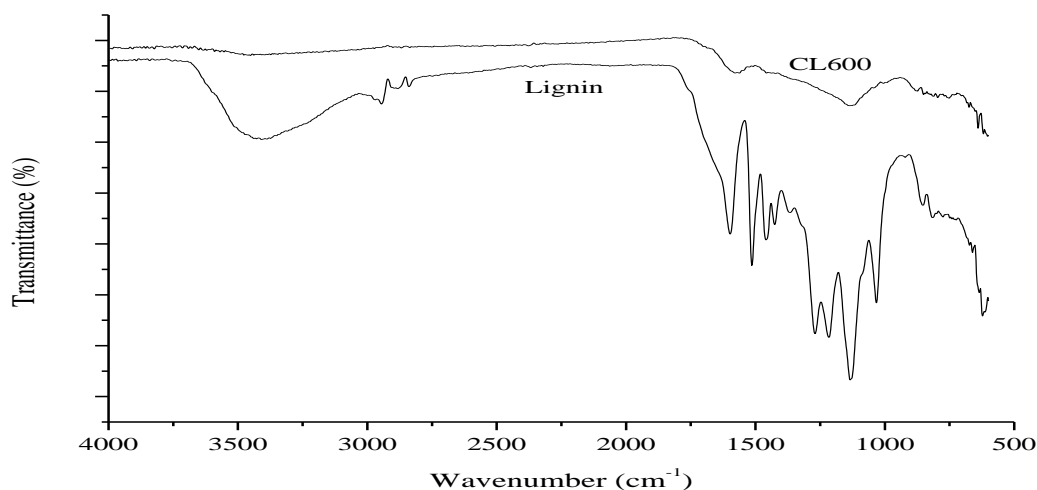


Figure 2: Infrared spectra for lignin and lignin char

The three bands at 2972, 2945 and 2880 cm^{-1} wavenumber levels correspond to the $\nu(\text{C-H})$ stretching vibrations (table 2) in aromatic methoxyl groups and in methylene groups of side chains [24, 25, 28, 29, 34]. The asymmetric and symmetric vibrations of deformation in plane of CH_3 group are respectively located at 1444 and 1361 cm^{-1} [24, 25, 28, 29, 34]. The band recorded at 1444 cm^{-1} can also be attributed to the vibration of deformation in plane of CH_2 group [24, 25, 28, 29, 34]. The C-H out-of-plane vibration ($\gamma(\text{C-H})$) in benzene causes the bands at 843 and 796 cm^{-1} [24, 25, 28, 29, 34].

The band appearing at 1740 cm^{-1} was attributed to the stretching vibration of the carbonyl groups $\nu(\text{C=O})$. The stretching vibration for $\nu(\text{C=C})$ in aliphatic chain causes the shoulder at about 1640 cm^{-1} while the skeletal C=C vibrations in aromatic rings, they are represented by four bands at about 1593, 1565, 1509 and 1454 cm^{-1} [24-26, 28, 29, 34].

In terms of $\nu(\text{C-O})$ stretching vibrations, the band at 1269 cm^{-1} could be attributed to the cyclic ether groups [25, 26, 28, 29] and that at 1204 cm^{-1} to the phenol groups and / or cyclic ethers [25, 26, 28, 29]. The peak at 1120 cm^{-1} is assigned to $\nu(\text{C-O})$ of the secondary alcohol ($-\text{R}_2\text{CH-OH}$) and / or aliphatic ether [25, 28, 29] while that at 1018 cm^{-1} to $\nu(\text{C-O})$ of the primary alcohol (R-OH) [25, 28, 29].

Table 2: Functional groups and corresponding band frequencies in the ATR spectra of lignin and lignin which has undergone various treatments

Lignin	ATR vibrational frequency (cm^{-1})					Functional groups
	CL600	CL600 (140°C,6h,air)	CL600 (245°C,6h,air)	CL600 (700°C,1h,CO ₂)	CL600 (245°C,6h,air) (700°C,1h,CO ₂)	
3410	3438	3370 3278	3398	3407	3370	$\nu_{\text{ass}}(\text{O-H})$
2972	-	-	-	-	-	$\nu^{\text{as}}_{\text{CH}_3}$
2945	-	-	-	-	-	$\nu^{\text{as}}_{\text{CH}_2}$
2880	-	-	-	-	-	$\nu^{\text{s}}_{\text{CH}_3}$ and/or $\nu^{\text{s}}_{\text{CH}_2}$
1740	-	-	-	1722	-	$\nu(\text{C=O})$
-	-	1713	1713	1713	-	
-	-	1695	1695	1695	-	
1640	-	1639	-	-	-	$\nu(\text{C=C})$ aliphatic
1593	1593	1593	1593	1593	1583	$\nu(\text{C=C})$ aromatic
-	1574	1574	-	1574	-	
1565	1556	1556	-	1556	1556	
-	1537	1537	1528	1528	-	
1509	-	1518	-	-	-	
-	-	1472	1472	1472	1472	
1454	1454	1454	-	1454	-	
1444	-	-	-	-	-	$\delta^{\text{as}}_{\text{CH}_3}$ and δ_{CH_2}
1417	1417	1407	1426	1400	-	$\delta(\text{O-H})$
1361	-	-	-	-	-	$\delta^{\text{s}}_{\text{CH}_3}$
-	-	-	-	1287	-	$\nu(\text{C-O})$
1269	1269	-	1269	1269	1260	
-	-	1250	1250	1250	1250	
-	-	1232	1232	-	-	
1204	1204	-	-	1185	-	
-	-	1139	1139	-	1148	
1120	1120	1120	1120	1120	1111	
1083	1083	1065	1065	1083	1074	
-	-	-	-	1046	1056	
1018	1018	-	1018	1018	-	
-	991	991	-	-	-	
-	981	982	-	-	-	
954	945	-	935	963	945	
907	907	-	-	-	-	
-	-	889	889	889	880	$\gamma(\text{C-H})$
-	851	-	-	861	861	
843	843	843	843	-	843	
796	796	796	796	815	-	
-	750	750	750	750	-	
-	-	685	685	-	-	$\gamma(\text{O-H})$
667	667	667	667	667	667	

Compared to the spectrum of the raw lignin, that of lignin char (CL600) presents an enlargement of infrared bands with a decrease in intensity and a concomitant loss of resolution (figure 2). This is due to the thermal

treatment of the lignin. Indeed, the carbonization is accompanied by a loss of mass and the development of a plastic phase by crazing [3, 4]. A reaction scheme for the thermal degradation of lignin and resulting products is proposed in the literature [38]. The formation of the plastic phase is revealed by electron microscopy characterization [3, 4]. The formation of this phase makes the amorphous material as shown in the X-ray diffractogram that we have achieved (Figure 3). Indeed, the diagram shows the broad peak centred at 22° and does not exhibit a horizontal basic line. This shows that the major part of the matter is amorphous and visualizes a very low order of crystallinity of the sample.

The decrease in the intensity of the $\nu(\text{O-H})$ stretching vibration is due to a significant loss of phenolic and alcoholic oxygenated groups [24, 26, 29]. The loss of these groups during the carbonization occurs in all biomasses [12-15, 19, 21, 22, 24, 26, 29, 36]. This loss indicates that these functional groups are thermally unstable [12-14].

Moreover, the bands corresponding to the stretching vibrations of the methyl and methylene groups are not discernable in the char. In fact, the loss of these groups is in favor of a decrease in aliphaticity [13, 15, 19, 24, 27, 29, 36] and an increase in aromaticity [12, 13, 15, 24, 29, 36]. The development of this latter is supported by the increase in the intensity of the aromatic out-of-plane deformation $\gamma(\text{C-H})$ and by the appearance of new absorptions at 851 and 750 cm^{-1} [12, 13, 24, 29].

As regards the $\nu(\text{C=C})$ vibration, the band at 1640 cm^{-1} assigned to the aliphatic functional groups disappears [13, 15, 36]. However, the skeletal vibrations $\nu(\text{C=C})$ in the aromatic rings which existed in lignin persist in the char [12, 13, 19, 36] with a slight displacement of the bands either to low or to high frequencies (table 2). In this regard, no explanation is advanced in the literature [24, 29].

Finally, the $\nu(\text{C-O})$ vibrations of raw lignin persist in char however with the appearance of new bands (table 2). These latter are characteristics of $\nu(\text{C-O})$ of the cyclic ether group involved in the formation of oxygen bridges (C-O-C) by polycondensation and polymerization [29, 36]. Comparing band intensity of the different oxygenated groups, ether group is more thermally stable than OH and OCH_3 groups. This is consistent with the work of Sharma and al. [29], Pastor-Villegas and al. [12] and Jaramillo and al. [17]. According to these authors, the ether oxygen provides the link between the aromatic layers formed during the carbonization.

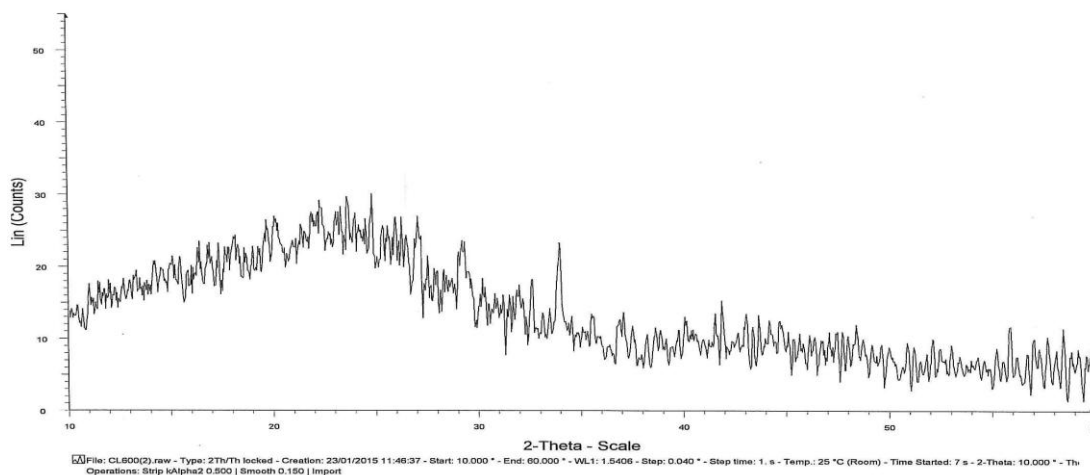


Figure 3: X ray diffractogram of lignin char

3.2. Effect of pre-oxidation

Figure 4 contains the infrared spectra of CL600, CL600(140°C ,6h,air) and CL600(245°C ,6h,air).

Compared to the spectrum of CL600, that of CL600(140°C ,6h,air) has a better resolution of the bands as well as increasing their intensity. The introduction of air would be in favor of a reduction of the plasticity. The same observation was made both with measurements of dimensional variations and also with the scanning electron microscope characterization [4].

The $\nu(\text{O-H})$ stretching vibrations, most of which the major part had disappeared during the carbonization reappear at 3370 and 3278 cm^{-1} following the coal treatment by the air.

The spectrum of CL600(140°C,6h,air) shows a shoulders at 1713 and 1695 cm^{-1} assigned to the $\nu(\text{C}=\text{O})$ vibration in the carbonyl groups formed during the pre-oxidation. The same result was obtained by Wang and al. [7], Lu and al. [11] and Calvillo and al. [39].

The $\nu(\text{C}-\text{O})$ stretching vibration bands assigned to the primary alcohol (1065 cm^{-1}), secondary and / or aliphatic (1120 cm^{-1}) and those of the cyclic ether (982 and 991 cm^{-1}) increased to intensity. The pre-oxidation promote the formation of oxygen bridges too.

For the rest of the spectrum, the bands are almost identical to those observed for CL600 with however a change of intensity.

Compared to the spectrum of CL600(140°C,6h,air), the bands of the spectrum of CL600(245°C,6h,air) have better resolution and a high intensity. This is partly due to the effect of temperature. This effect is also very pronounced at 1593 cm^{-1} , band assigned to $\nu(\text{C}=\text{C})$ aromatic groups. Under these conditions, the sample aromaticity was improved.

Moreover, in so far as the resolution and the intensity of bands for the different oxygenated complexes were improved, the plasticity of the sample was thereby reduced. However, the intensity of OH group decreases when oxidation temperature increases (figure 4). The same result was obtained by Worasuwanarak and all. [8] and by Cimadevilla and all. [9]. The decrease of the OH band intensity would be due to the dehydration and / or to the oxidation of hydroxyl groups into carboxyl and aldehyde groups. The formation of the latter would be the origin of the increase in the $\nu(\text{C}-\text{O})$ band (figure 4). Finally, the band observed at 982 cm^{-1} attributed to the $\nu(\text{C}-\text{O})$ vibration of the cyclic ether completely disappears by a treatment at 245°C. This would indicate that the increase in the pre-oxidation temperature leads to the opening of the cyclic ether corresponding to the aforementioned band. Note that the different $\nu(\text{C}-\text{O})$ vibrations recorded from spectra reveal the existence of several types of cyclic ether.

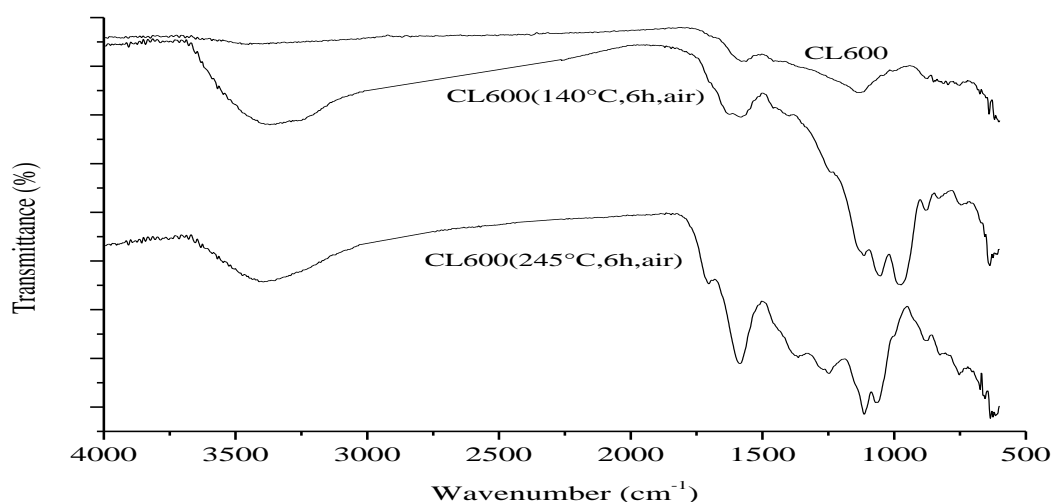


Figure 4 : ATR spectrum of lignin char and pre-oxidized samples

3.3. Effect of activation

Figure 5 includes the infrared spectra of CL600, CL600 (700°C, 1h, CO₂) and CL600 (245°C, 6h, air) (700°C, 1h, CO₂).

The general appearance of CL600 (700°C,1h,CO₂) spectrum is the same as that of CL600. The activating effect is manifested by a good resolution of the bands. In the 1720-1690 cm^{-1} range, the three new bands located at 1722, 1713 and 1695 cm^{-1} are attributed to $\nu(\text{C}=\text{O})$ stretching vibrations. The presence of these vibrations indicates that CO₂ reacts with carbon to form carbonyl groups. The same result was obtained by Yang and al. [13] and Guo and al. [14]. According to Perezdrienko and al. [40], the oxidation of a part of alcoholic hydroxyl groups to carboxyl and aldehyde is the cause of the progressive increase of the intensity of the $\nu(\text{C}=\text{O})$ absorption band during activation. The formation of carbonyl groups leads to decrease of the thermoplastic character and to development of porosity. This also appears clearly in images taken by TEM (Figure 6). At the end, the increase of the intensity of $\nu(\text{C}=\text{C})$ vibration bands between 1600 and 1450 cm^{-1} suggests the enhancement of the aromatic character of material [13].

The infrared spectrum of CL600 (245°C, 6h, air) (700°C, 1h, CO₂) is compared with that of CL600 (700°C, 1h, CO₂). The characteristic bands of $\nu(\text{C}=\text{O})$ group disappear and the majority of vibration bands expand. It would thus seem that activation by CO₂ preceded by a pre-treatment in air leads to the development of new thermoplastic character but with a degree less than that of CL600. This finding is further highlighted by the characterization made by a transmission electron microscope (TEM) (Figure 6).

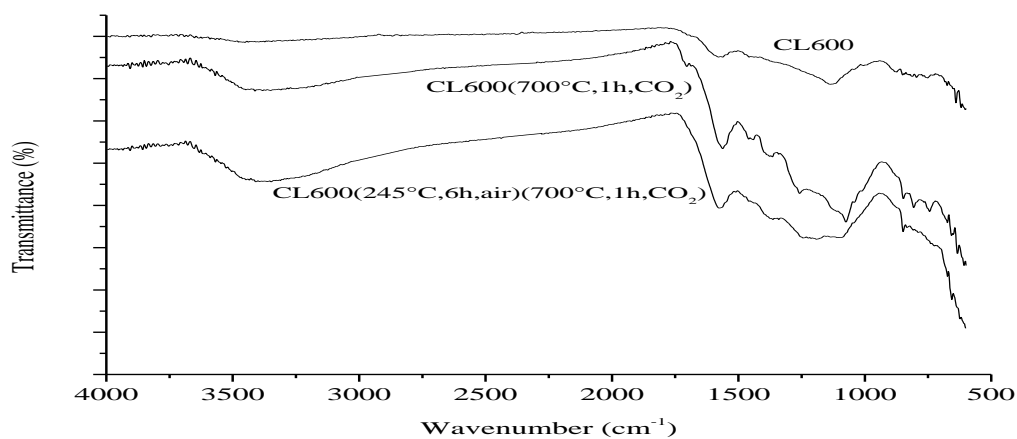


Figure 5: ATR spectra of lignin char and activated samples

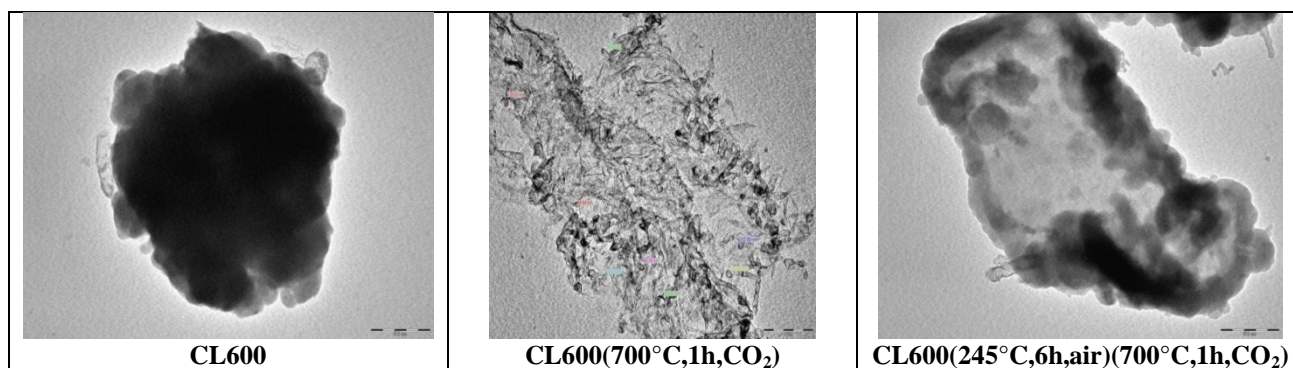


Figure 6: Images taken by TEM of lignin char and activated samples

TEM images displayed in this figure show that the CL600 (700°C,1h,CO₂) compound has better porosity than the CL600 (245°C,6h,air) (700°C,1h,CO₂) compound.

Conclusion

1. In the present work, the ATR infrared spectroscopy was used for the characterization of the lignin and derivatives chars.
2. The main oxygenated groups present in lignin are the aliphatic and cyclic ether, methoxyl, carbonyl, phenolic hydroxyl, primary and secondary aliphatic hydroxyl groups.
3. Carbonization is accompanied by a significant loss of oxygen groups except the cyclic ether group, the aromatization of structure and the forming of a plastic phase by crazing. The bands for the different oxygenated groups intensified during the pre-treatment of coal by air.
4. The pre-treatment in air also leads to the formation of the carbonyl group. The presence of all these groups and increasing the pre-treatment temperature is reflected by a decrease of the thermoplastic character of the material.
5. During activation of the raw char, the reappearance of C=O groups derived from carbon dioxide reactions with the carbon matrix. These groups do not appear when activating is preceded by the pre-oxidation of coal.
6. Images taken by TEM demonstrate the development of porosity when the activation is performed on the raw coal and the formation again of the plastic phase when activation is preceded by a pre-treatment.

References

1. Jankowska H., Swiatkowski A. and Choma J., *Active Carbon*, Ed. Ellis Horwood Limited, London (1991) 75.
2. Wan W.M.A. Daud and Houshamnd A.H., *J. Nat. Gas Chem.* 19 (2010) 267.
3. Kifani-Sahban F., Kifani A., Belkbir L., Zoulalian A., Arauso J., Cordero T., *Thermochim. Acta* 298 (1997) 199.
4. Sebbahi S., Ahmido A., Kifani-Sahban F., El Hajjaji S., Zoulalian A., *J. Eng.* 2014 (2014) Article ID 972897, 1.
5. Zhu Y., Gao J., Li Y., Sun F., Gao J., Wu S. and Qin Y., *J. Taiwan Instit. Chem. Eng.* 43(1) (2012) 112.
6. Nowicki P., Pietrzak R. and Wachowska H., *Fuel* 87 (2008) 2037.
7. Wang Q.-B., Zhang X.-L., Xu D.-P. and Chen Q.-R., *J. China Univ. Mining Technol.* 17(4) (2007) 494.
8. Worasuwanarak N., Hatori S., Nakagawa H. and Miura K., *Carbon* 41(5) (2003) 933.
9. Cimadevilla J. L. G., Alvarez R. and Pis J. J., *Fuel Process. Technol.* 87(1) (2005) 1.
10. Mourao P. A. M., Laginhas C., Custodio F., Nabais J. M. V., Carrott P.J.M. and Carrott M. M. L. R., *Fuel Process. Technol.* 92(2) (2011) 241.
11. Lu C., Xu S., Wang M., Wei L., Liu S. and Liu C., *Carbon* 45(1) (2007) 206.
12. Pastor-Villegas J., Meneses Rodríguez J.M., Pastor-Valle J.F., Rouquerol J., Denoyel R. and García García M., *J. Anal. Appl. Pyrol.* 88 (2010) 124.
13. Yang T. and Lua A.C., *J. Colloid Interf. Sci.* 267 (2003) 408.
14. Guo J. and Lua A. C., *Mater. Lett.* 55 (2002) 334.
15. Bouchelta C., Medjram M.S., Bertrand O. and Bellat J.-P., *J. Anal. Appl. Pyrol.* 82 (2008) 70.
16. Cetinkaya S. and Yurum Y., *Fuel Process. Technol.* 67 (2000) 177.
17. Jaramillo J., Álvarez P. M. and Gómez-Serrano V., *Fuel Process. Technol.* 91 (2010) 1768.
18. Matos J., Nahas C., Rojas L. and Rosales M., *J. Hazard. Mater.* 196 (2011) 360.
19. Zhang J., Fu H., Lv X., Tang J. and Xu X., *Biomass Bioenergy* 35 (2011) 464.
20. Demiral H., Demiral I., Karabacakoglu B. and Tümsek F., *Chem. Eng. Res. Design* 89 (2011) 206.
21. Li W.-H., Yue Q.-Y., Gao B.-Y., Wang X.-J., Qi Y.-F., Zhao Y.-Q., Li Y.-J., *Desalination* 278 (2011) 179.
22. Nabais J.M.V., Nunes P., Carrott P.J.M., Carrott M.M.L.R., García A.M., Díaz-Díez M.A., *Fuel Process. Technol.* 89 (2008) 262.
23. Song M., Jin B., Xiao R., Yang L., Wu Y., Zhong Z. and Huang Y., *Biomass Bioenergy* 48 (2013) 250.
24. Maldhure Atul V. and Ekhe J.D., *J. Environ. Chem. Eng.* 1 (2013) 844.
25. Savy D. and Piccolo A., *Biomass BioEnergy* 62 (2014) 58.
26. Carrott Suhas, P.J.M. and Ribeiro Carrott M.M.L., *Bioresour. Technol.* 98 (2007) 2301.
27. Hu J., Shen D., Wu S., Zhang H. and Xiao R., *J. Anal. Appl. Pyrol.* 106 (2014) 118.
28. Sun Y.-C., Xu J.-K., Xu F. and Sun R.-C., *Ind. Crops Prod.* 47 (2013) 277.
29. Sharma R.K., Wooten J.B., Baliga V.L., Lin X., Chan W. G. and Hajaligol M.R., *Fuel* 83 (2004) 1469.
30. Fathy N. A., Sayed Ahmed S. A. and Abo El-enin R.M.M., *Environ. Res. Eng. Manag.* 1(59) (2012) 10.
31. Allwar A., *Inter. J. Res. Chem. Environ.* 3(2) (2013) 62.
32. Marković J.P., Radović J.B., Štrbanović R.T., Bajić D.S., Vrvic M.M., *J. Serbian Chem. Soc.* 74(8-9) (2009) 885.
33. Bykov I., Master Thesis, Division of Chemical Technology Department of Chemical Engineering and Geosciences Lulea University of Technology S-971 87 Lulea (2008).
34. Boeriu C.G., Bravo D., Gosselink R.J.A. and Van Dam J.E.G., *Ind. Crops Prod.* 20 (2004) 205.
35. Sheet E. M., Sheet M. S. and Hamed A.Y., *Mesopotamia J. Agric.* 35(1) (2007).
36. Gomez-Serrano V., Piriz-Almeida F., Duran-Valle C.J., Pastor-Villegas J., *Carbon*, 37(10) (1999) 1517.
37. Silverstein, Webster and Kiemle, Identification spectrométrique de composés organiques, 2^{ème} édition, De Boeck (2007).
38. Brebu M. and Vasile C., *Cellulose Chem. Technol.* 44(9) (2010) 353.
39. Calvillo L., Moliner R. and Lázaro M.J., *Mater. Chem. Phys.* 118 (2009) 249.
40. Perezdrienko I.V., Molodozhenyuk T.B., Shermatov B.E., Yunusov M.P., *Russian. J. Appl. Chem.* 74 (2001) 1650.